This is the Submitted Manuscript version of an article accepted for publication in Nature Nanotechnology. Küchler, A., Yoshimoto, M., Luginbühl, S. et al. Enzymatic reactions in confined environments. Nature Nanotech 11, 409–420 (2016). https://doi.org/10.1038/nnano.2016.54

# Enzymatic Reactions in Confined Environments

Andreas Küchler[1], Makoto Yoshimoto[2], Sandra Luginbühl[1], Fabio Mavelli[3], Peter Walde[1]*

[1] Department of Materials, ETH Zürich, Vladimir-Prelog-Weg 5, CH-8093 Zürich, Switzerland

[2] Department of Applied Molecular Bioscience, Yamaguchi University, Tokiwadai 2-16-1, Ube 755-8611 Japan

[3] Chemistry Department, University "Aldo Moro", Via Orabona 4, 70125 Bari, Italy

## Abstract

Within each biological cell, surface- and volume-confined enzymes control a highly complex network of chemical reactions. These reactions are efficient, timely, and spatially defined. Efforts to transfer such appealing features *in vitro* have led to several successful examples of chemical reactions catalysed by isolated enzymes. In most cases, enzymes are either bound or adsorbed to an insoluble support, or physically trapped in a macromolecular network or encapsulated within compartments. Advanced applications of enzymatic cascade reactions with immobilized enzymes include enzymatic fuel cells and enzymatic nanoreactors, both for *in vitro* as well as for possible *in vivo* applications. In this Review, we discuss some of the general principles of enzymatic reactions confined on surfaces, at interfaces and inside small volumes. We also highlight the similarities and the differences between the *in vivo* and *in vitro* cases and attempt to critically evaluate some of the necessary future steps to improve our fundamental understanding of these systems. (154 words)

For many years, the structure, stability, and catalytic properties of water-soluble enzymes have been studied by analysing their crystal structures and by investigating how enzymes behave as catalysts when dissolved at a certain concentration in a buffered aqueous solution of defined composition and temperature. In this way, characteristic *in vitro* features of individual, purified enzymes could be elaborated and mechanisms were formulated for explaining the enzymes' ability of catalysing a particular type of chemical reaction[1,2]. Such studies have shown that *substrate binding* and an intact *active site* are essential for the proper functioning of enzymes as *dynamic* globular macromolecules[3]. However, a simple buffer solution does not reflect the compositional complexity of the biological medium in which enzymes normally perform. Most *in vivo* enzyme-catalysed reactions occur in a molecularly crowded environment[4] and/or in a confined environment, such as on a surface, at an interface, or inside a small volume[5-7]. These factors – among others − have to be taken into account if one likes to synthetically imitate the *in vivo* environment of the enzymes of interest, or if one aims at better understanding altered behaviour of isolated enzymes in *in vitro* applications.

In this conceptual review we will focus on a few aspects of confined enzymatic reactions both *in vivo* and *in vitro.* We will refer to examples of enzymes which perform in confined environments *in vivo*; and we will present some general features and selected examples of *in vitro* reactions catalysed by volume- and surface confined (immobilized) enzymes. Particular attention will be paid to *in vitro* enzymatic cascade reactions with different types of enzymes which catalyse sequential multi-step reactions[6,8-10]. Furthermore, selected applications of immobilized enzymes will be discussed, with particular emphasis on applications where the defined confinement of enzymatic reactions to either a surface or a volume appears advantageous.

*In vitro surface- and volume-confined enzymatic reactions* with isolated, immobilized enzymes are often carried out not only for understanding the *in vivo* behaviour of enzymes, but also for elaborating the possibilities for *in vitro* applications. Indeed, analytical and biotechnological applications of immobilized enzymes exist for the preparative modification, degradation or synthesis of organic molecules[1,11-14]. Immobilizing enzymes on surfaces or in confined volumes often allows for a facile separation of the enzymes from the reaction products[3], a key advantage with respect to reactions with dissolved enzymes. More

sophisticated systems can involve enzymatic cascade reactions, in which the relative spatial localization of the enzymes is a prominent aspect, both for *in vitro* applications and for characterizing *in vivo* systems[6,13].

For *surface-confined* enzymatic reactions, the enzymes are either adsorbed or bound to a support *via* non-covalent or covalent bonds. For *volume-confined* enzymatic reactions, the enzymes are physically entrapped either within a macromolecular network or within compartments. In this latter case, the substrate molecules have to be able to access the enzymes from the external medium or from other compartments, unless the substrate molecules already are present within the compartment from the beginning.

Conceptually, there are obvious similarities between confined *in vivo* and *in vitro* enzymatic reactions. However, there are also noticeable differences. One significant difference is that in biological systems new enzymes are constantly synthesized to replace the ones that have been released, inactivated or degraded[15], whereas in non-living *in vitro* systems, there is no such continuous *de novo* synthesis. Furthermore, the efficiency of multi-enzyme complexes[6,13] with a spatially defined localization of different types of enzymes with their specific substrate channelling is difficult to achieve outside cells. Hence, enzymes extracted from biological samples and applied *in vitro* cannot compete with the *in vivo* situation if long-term performance and efficiency of enzymatic cascade reactions are considered. Consequently, any type of application of immobilized enzymes requires not only an optimal enzyme localization but also an optimization of the enzymes' storage and operational stabilities[1,11,16].

Despite these limitations, and the fact that enzymes are intrinsically unstable, confined enzymes can still be powerful *in vitro* catalysts for the following two seemingly contradictory reasons: First, enzymes often catalyse chemical reactions regio- and stereoselectively with high substrate specificity[1,2]. Thus, a high selectivity can be achieved which is hard to attain using traditional organic chemistry approaches. On the other hand, many enzymes exhibit low specificity (*e.g.* lipases, oxidative enzymes), which also allows them to be used for catalysing transformations of completely synthetic, non-natural substrates[17-21]. Moreover, enzymes from different host organisms can be combined *in vitro,* which makes it possible to create enzymatic cascade reactions that do not occur in biological systems[22]. (738 words)

## 1. Enzymatic reactions confined on surfaces or at interfaces

Many enzymatic reactions in living systems take place in biological membranes[5,6,23]. The study of these surface- or interface-confined enzymatic reactions *in vivo* has inspired the use of various *in vitro* systems which mimic the lipid matrix of biomembranes in the form of lipid vesicles[24-26], reversed micelles[27-29], or solid supported lipid bilayers[30,31].

Apart from these bio-mimicking approaches, enzymatic reactions occurring on non-natural surfaces have been studied and applied for many years. **Fig. 1** schematically illustrates some of the possibilities of immobilizing isolated enzymes on solid or soft supports in order to conduct surface-confined enzymatic reactions *in vitro*. In all cases, the immobilized enzymes are exposed to the bulk aqueous solution in which the substrate molecules are dissolved. The substrate accessibility to the active site of an enzyme may be restricted by physical constraints, for example when the enzymes are adsorbed in the pores of mesoporous particles or in the inner part of a hydrogel, or when the active site faces the surface of the support instead of the bulk solution. One of the main advantages of immobilizing enzymes on insoluble solid supports is that the products at the end of the reaction are easy to collect, provided they are still soluble [1,2,11]. This permits the construction of surface-confined enzymatic reactions in flow reactor systems (*e.g.*, microfluidic chips[32,33] or nanochannels[34]). The immobilization of enzymes on solid supports often results in a lower catalytic activity than in bulk solution, because immobilization leads to a decrease in conformational flexibility[35], but frequently in a higher operational stability than in bulk solution[11].

Conceptually, there are different ways of immobilizing enzymes – or any other types of proteins − on solid supports[1,11,12,14,36,37]. Apart from simple adsorption (**Fig. 1a**), often, the support is first modified with small organic linkers with reactive functional groups (**Fig. 1b**). The linkers are exposed to the bulk solution for a direct, covalent attachment of the enzymes to the surface. Alternatively, the solid support is first coated with an organic layer to which the enzymes are covalently bound (**Fig. 1c-e**), again through linker molecules. Such soft organic coating prevents enzyme inactivation that might occur in case of direct contact with the solid support (**Fig. 1a**). The coating may consist of adsorbed or covalently bound self-

assembled monolayers (**Fig. 1c**) or bilayers (**Fig. 1d**) of amphiphilic molecules, globular proteins (bovine serum albumin, avidin)[36] or polymers (**Fig. 1e**)[32,38]. Another possibility is to adsorb large dendronized polymer-enzyme conjugates, previously prepared in solution (**Fig. 1f**).[33, 39] In some cases, enzymes immobilized on a surface can be more stable than in bulk solution[11]. However, it is still unclear how to quantitatively describe enzymatic reactions with surface-bound enzymes[1,2], since the precise concentration of bound enzymes is difficult to determine, and since the enzymes are fixed on a solid support (no three-dimensional diffusion) while the substrate molecules diffuse in the entire volume.

One exciting perspective is that different types of enzymes can be immobilized in a precise and sequential way to design *multi-step cascade reactions* (specific examples are shown in **Fig. 2a-d**)[6,8 9,13,38,39]. A fine spatial control may speed-up the reaction, reduce unwanted side reactions, and decrease the accumulation of inhibitory or reactive intermediates[6,13]. In order to do so, one particular concept is illustrated in **Fig. 2a**. Biotinylated glucose oxidase (GOD) and horseradish peroxidase (HRP) are bound to biotinylated DNA origami building blocks with the help of neutravidin to form a dimer nanoreactor[40].

Based on geometrical considerations, the active sites of two co-immobilized enzymes which catalyze two consecutive reactions should not be further away from each other than 0.1 -1 nm[41]. However, this prediction appears to contradict experimental results in that it was found that such a close proximity of two enzymes is not necessary for an increase in the reaction efficiency in comparison to free enzymes (**Fig. 2b**)[42]. This apparent discrepancy can be explained by considering that substrate channeling between enzymes positioned further away from each other than 1 nm is possible if the local *density* of the two (or more) enzymes involved in the cascade reaction is over a certain threshold ('enzyme cluster-mediated channeling')[41]. Placing GOD and HRP *via* DNA origami tiles at a distance of 10 nm from each other leads to a significant activity increase in comparison to the free enzymes and in comparison to being placed 20, 45, or 65 nm apart (**Fig. 2b**)[42]. This activity increase could be due to an efficient migration (channelling) of the reaction intermediate ($H_2O_2$) from the active site of GOD to the active site of HRP through the hydration layer on the surface of the two enzymes. Substrate channelling occurs in living systems too, specifically in membrane-bound multi-enzyme complexes (also called "enzyme super-complexes" or "metabolons"[6]), for example in the case of the eight-enzyme complex responsible for the citric acid cycle[43]. In

this particular case, substrate channelling between the active sites is likely to be due to electrostatic interactions on the surface of the enzymes[43]. Apart from this sequestration mechanism, covalent tethering, *i.e.* the covalent binding of substrates and intermediates to the enzymes, is an alternative way of *in vivo* substrate channelling[44].

The example illustrated in **Fig. 2c** shows a completely different way of co-localizing GOD and HRP, but with much lower positional precision and a much less sophisticated approach than in the case of the DNA-origami systems of **Fig. 2a** and **2b**. GOD was adsorbed inside mesoporous silicate particles, and HRP was placed on top of the particles *via* a HRP-polymer conjugate to form a two-enzyme system of high storage stability[45].

Another example of an *in vitro* cascade reaction involves three enzymes implicated in the menaquinone biosynthetic pathway (**Fig. 2d**)[46]. The enzymes were randomly immobilized on CdSe-ZnS core/shell quantum dots with a diameter of 3.5 nm. The efficiency of the cascade reaction depended on (i) the total number of enzymes per particle, and (ii) the relative ratio of the three enzymes per particle [46]. This study demonstrates the importance to co-localize the three enzymes as well as the importance of the inter-enzyme distance. Since the enzymes were tightly packed on the quantum dots surface, it is unlikely that the surface itself had an effect on the behaviour of the enzymes and only served as a scaffold for bringing the different enzymes in close proximity. Interestingly, however, nanoparticle-confined enzymes may show enhanced activity compared to freely diffusing enzymes, even if only one type of enzyme is used (no cascade reaction)[35]. For example, chymotrypsin immobilized on modified gold nanoparticles showed enhanced catalysis depending on the charge of the substrates, indicating the influence of the microenvironment of the immobilized enzyme on the reaction[47].

Using surface confined enzymes force cascade reactions to occur close to the surface of the support, thus enabling applications in which *the surface itself* plays an active role, as in the case of enzymatic fuel cells[48-53] or electrochemical biosensor devices, both involving redox enzymes. Examples include *in vivo* power generators that use glucose in the blood as a fuel[54], or sensors for measuring the glucose concentration in blood[55]. In these devices [48-55], a steady flow of electrons occurs between the supporting electrode and the immobilized redox enzymes. The reactions must take place close to the electrode surface, and the active site of the enzymes must have the correct orientation. The electron exchange between

enzyme and electrode can occur either directly or through a conductive small molecule, polymer or particle[54]. In order to achieve appreciable current densities, nanostructured electrodes with a high surface area are usually used. Such electrodes can be prepared from conductive carbon-based materials (carbon nanotubes or graphene) or from conductive polymers.

One recent example of an enzymatic fuel cell comprised an oxidative enzyme (deglycosylated flavin adenine dinucleotide-dependent glucose dehydrogenase, d-FAD-GDH) immobilized on a nanostructured anode surface (magnesium oxide-templated mesoporous carbon) (**Fig. 3a)**[56]. The adsorption of d-FAD-GDH on the electrode surface was achieved by adding the enzyme to a hydrogel coating consisting of an electrically conductive polymer containing an osmium complex that can undergo a redox reaction[57] and a crosslinker poly(ethylene glycol) diglycidyl ether. Using this configuration, current densities as high as 100 $mA/cm^2$ were obtained at the anode as a result of the oxidation of 0.5 M glucose at pH=7.0 [56].

Another example of a confined enzymatic reaction *in vitro* is the polymerisation of aniline on the surface of anionic vesicles (**Fig. 3b)**. HRP and $H_2O_2$ react with aniline on the vesicle surface[58] to form the emeraldine salt form of polyaniline (PANI-ES). This is an example which relies on the fact that the peroxidase can oxidize non-natural substrates (aniline). Aniline monomers adsorb from the bulk aqueous solution onto the vesicle membranes, and during the course of the reaction the intermediates and products bind to the vesicle surface, where the enzyme is also localized[58]. The vesicles act as reaction regulator in that the outcome of the reaction is influenced by the vesicles in a positive way (formation of the desired PANI-ES)[58,59]. (1470 words)

## 2. Enzymatic reactions in confined volumes

Volume-confined enzymatic reactions are also common in biological systems[5,23,60]. In eukaryotes, for examples, endosomes (typically 100-500 nm in diameter[61]) host degradative reactions carried out by about 40 different hydrolytic enzymes, which in turn are contained

inside smaller lysosome vesicles[5]. The membrane of endosomes consists of amphiphilic lipids and various embedded proteins that separate the inside environment with a pH of ~5, where degradative enzymes work best, from the cytoplasm, at pH=7.2. Other examples of volume-confined enzymatic reactions in eukaryotes can be found in mitochondria (~0.5-5μm in diameter) and peroxisomes (~500nm in diameter[5,61]). A particularly useful and much investigated system is the carboxysome, a confined environment found in certain type of prokaryotes where carbon fixation from $CO_2$ is carried out[23,60,62-64].

Carboxysomes are icosahedral compartments of 100-200 nm in diameter separated from the cytoplasm by a membrane consisting only of proteins, with a thickness of about 2-3 nm[65]. They contain only two types of enzymes: CsoSCA (carboxysome shell carbonic anhydrase) and RuBisCO (ribulose-1,5-bisphosphate carboxylase/oxygenase)[65-67] that are specifically localized to optimize a two-step cascade reaction[63]: Conversion of bicarbonate ($HCO_3^-$) to $CO_2$ and $H_2O$, catalyzed by CsoSCA, and subseqent carboxylation of ribulose-1,5-bisphosphate with the formed $CO_2$, catalyzed by RuBisCO, to yield two molecules of 3-phosphoglycolate, *i.e.* products in which the C-atom of $CO_2$ is incorporated (corresponding to the first major step in carbon fixation)[63]. In *Halothiobacillus neapilitanus*, for example, each carboxysome contains about 40 copies of CsoSCA[65,66], attached to the inner surface of the protein shell, and about 270 copies of RuBisCO, in the interior of the compartment[23,63,65,67]. This example illustrates that the localization and the number of enzymes in each compartment are key parameters that need to be taken into account to ensure optimal reaction efficiency in volume-confined systems.

**Figure 4** shows a schematic representation of various types of confined environments in which enzymes can be localized for catalysing reactions *in vitro*. They include reverse micelles (**Fig. 4a**), water-in-oil droplets (**Fig. 4b**), vesicles (**Fig. 4c**), protein cages (**Fig. 4d**), polymer capsules (**Fig. 4e**), and arrays of small reaction vessels (**Fig. 4f**). A characteristic feature of all these compartments is the high ratio of interfacial (surface) area to volume, which may vary from $10^9$ $m^{-1}$ for a 5 nm water pool in a reverse micelle (**Fig. 4a**) to $10^5$ $m^{-1}$ for a 50 μm giant vesicle (**Fig. 4c**). Therefore, possible boundary effects arising from interactions with the inner surface of the compartment become more pronounced the smaller the volume is. Volume-confined reactions of the type discussed here (**Fig. 4**) can occur in three conceptually different ways.

*First*, the enzymes and all reacting molecules are placed into the confined volume from the outset. In this case, the enzymatic reactions are expected to start during the preparation of the compartment systems, for example during the formation of vesicles (**Fig. 4c**)[68,69], or during the formation of water in oil (w/o) droplets (**Fig. 4b**)[70].

*Second*, substrate molecules are delivered to the enzyme by merging or transiently fusing compartments loaded with either component. Merging compartments, as in the case of vesicles[71] or w/o droplets[70], leads to an increase in the size of the confined volumes and at the same time to a decrease in the number of separated volumes. In the case of reverse micelle droplets (**Fig. 4a**), fusion and fission occurs continuously and without any significant change in the average size and number of water pools over time (provided that the volumes of the colliding compartments are the same)[27,28]. The kinetics of the enzymatic reactions in such dynamic systems is influenced by the collision and fusion kinetics; a robust, quantitative kinetic model for measuring reaction rates in these systems remains to be developed[27,28,72,73].

*Third,* water soluble substrates can be delivered to a volume-confined enzyme across the compartment boundary. This is how enzymes inside cells and inside their organellar subcompartments receive their substrates[5]. The reaction is dependent on the rate of substrate permeation across the boundary, which is determined by the chemical structures of the substrate and the boundary. Thus, the specificity of an enzymatic reaction can be controlled by the activity of the entrapped enzyme and by the vesicle shell permeability (**Fig. 4c**)[74,75], as is the case of protein capsules (**Fig. 4d)**[76,77].

Sophisticated examples of volume-entrapped enzymatic reactions include a biochemical oscillator confined to w/o droplets of 2-40 μm diameters [78], and a cell-free gene expression system confined into 3 μm deep poly(dimethylsiloxane) wells with a volume of 20 fL[79]. Most of the volume-confined reactions investigated so far were much simpler and have been localized in either reverse micelles, w/o microemulsions or in vesicles. Enzymatic reactions in reverse micelles are an interesting case because the number of water molecules within the core of a reverse micelle is very small. As a result, enzymes in reverse micelles can behave differently than in bulk aqueous solutions, although choosing proper conditions for a correct comparison of the two systems is not trivial [28]. Several reports indicate that some enzymes – for example chymotrypsin[80,81] or HRP[82,83] – appear to act more efficiently when confined in

reverse micelles than in bulk solution[27,80]. However, there still is no clear and general understanding of this enzyme "superactivity". It has been suggested that it may be due to conformational changes [27,80], to the particular local concentrations of enzyme and substrates, [73,80] or to the thermodynamic and kinetic properties of the confined water[82] that may lead to an altered hydration state of the active site of the enzyme [83]. It is likely that different effects play a role, depending on the type of enzyme, the chemical structures of the substrate and the amphiphiles forming the reverse micelle.

A simple but important geometric consideration arises in the case of enzymatic reactions inside vesicles. The larger the volume of the vesicle, the more the enzyme approaches bulk behaviour. This is simply because the volume to surface ratio of the vesicles increases with increasing volume. Consider a large unilamellar vesicle (LUV) with a diameter of 100 nm and a bilayer membrane thickness of 5 nm, as well as a giant unilamellar vesicle (GUV) with a diameter of 50 µm and a bilayer membrane thickness of 5 nm. If the LUV is scaled up to a sphere with a diameter of 10 cm, it will have a sphere shell thickness of 5 mm. Conversely, if the GUV is scaled up by the same amount, it will also have a sphere shell thickness of 5 mm but its diameter will be 50 m! In comparison, if a small monomeric enzyme with a diameter of 5 nm is also scaled up by the same amount, it will have a size of 5 mm. This exercise shows that from the point of view of the enzyme, the situation in a GUV is nearly identical to the situation in a bulk solution. Nevertheless, if complex enzymatic cascade reactions with *different types of enzymes* and substrates at low concentrations are considered, then a volume-confinement as large as a few µm can still have significant effects due to stochastic fluctuations in the volume composition (extrinsic stochasticity), and therefore in the volume properties (*i.e.*, the local concentrations of the different enzymes and substrates). Extrinsic stochasticity may result in significant differences between individual enzyme-containing compartments with respect to enzymatic reaction efficiency (*i.e.*, rate of product formation and product distribution). Such stochastic effects are expected to be more substantial the smaller the vesicles are and the lower the solute concentration is [84]. Simple calculations show that spherical vesicles with a diameter of 10 µm (corresponding to an internal volume of $5.2 \cdot 10^{-13}$ L) loaded with an enzyme at a concentration of 10 µM, contain on average $3.2 \cdot 10^{6}$ enzymes. On the other hand, 100 nm spherical vesicles (internal volume of about $5.2 \cdot 10^{-19}$ L) loaded with the same 10 µM enzyme solution, will on average contain only 3 enzymes. This means that under loading conditions which lead to a Poisson distribution of

the enzymes among a population of mono-dispersed vesicles, stochastic fluctuations are particularly relevant for populations of small vesicles[84]. It is worthwhile to remark that a Poisson distribution is theoretically expected for equally sized compartments only if the entrapment of molecules is solely driven by chance, that is, in the ideal case where solute-solute and solute-compartment boundary interactions are negligible. However, the difference becomes clearly more pronounced if *different types of enzymes* are loaded within such small vesicles, as both the total amount of enzyme molecules present in one vesicle and their relative ratio vary. This stochastic effect is expected to have significant consequences in the case of enzymatic cascade reactions, as there will be a large vesicle-to-vesicle variation[84]. For micrometer-sized volumes, one may expect that stochastic effects due to different enzyme loadings are less likely, although they have been observed experimentally in giant lipid vesicle-confined protein expression experiments involving more than 30 different enzymes[84-86]. These experiments indicate that the Poisson distribution based on an ideal solute behaviour is too simple for accurately describing more complex systems[87].

In spite of experimental difficulties with respect to the entrapment of enzymes in vesicles, a number of potential applications have been reported. One study is illustrated in **Fig. 5a**. Unilamellar phospholipid vesicles with a diameter of about 100 nm containing the degrading enzyme phosphotriesterase were prepared *in vitro* for *in vivo* application as a nanoreactor system which could circulate in the blood stream after appropriate injection[88] and hydrolyse neurotoxic organophosphorous compounds . These partially hydrophobic organophosphorous compounds permeate into the vesicles where the enzymatic hydrolysis into non-toxic products takes place. The vesicles protect the enzyme from inactivation by blood components. The hydrolysis products may accumulate inside the vesicles or leak out into the blood circulation. The residence time of the vesicles in the blood circulation depends on the vesicle membrane composition. Clearance of the vesicles by the immune system is expected to be slowed down by the presence of polyethyleneglycol (PEG) on the vesicle surface[89].

In another example, illustrated in **Fig. 5b**, GOD and catalase were co-entrapped inside 100 nm unilamellar phospholipid vesicles in which the membrane contained a porin transport protein[90]. The vesicles were covalently bound to chitosan gel beads and were used as an *in vitro* reactor for the conversion of D-glucose into glucono-δ-lactone, followed by the non-

enzymatic hydrolysis into gluconic acid. The migration of D-glucose from the bulk aqueous solution into the vesicles was promoted by the transport protein. The catalase protected the activity of the oxidase as it catalyses the degradation of $H_2O_2$, a side product of the oxidation reaction that inactivates the oxidase[90].

Vesicles are attractive systems to study enzymatic reactions mainly for two reasons: the large variability of their size and the possibility to design multiple vesicles systems. More specifically, depending on the preparation procedure, vesicle diameters can vary between ~30 nm (corresponding to a volume of $1.4 \cdot 10^{-20}$ L) to more than 300 µm (volume = $1.4 \cdot 10^{-6}$ L). Moreover, because vesicles do not spontaneously fuse or exchange their aqueous interiors, it is possible to create multi-vesicular systems in which large vesicles contain smaller vesicles in their interior. In principle, the chemical composition of any membrane in the system can also be changed by design. This large variability allows investigations of cascade reactions with enzymes that are located in different internal vesicles mimicking eukaryotic cells and their enzyme specific organelles[91].

Potential drawbacks arising from volume-to-volume variations like in the case of vesicles, for example two-enzymes-containing polymersomes (**Fig. 6a**)[92], are also expected for other compartment systems. In contrast, however, with specially designed protein capsules and mutant enzymes (**Fig. 6b** and **Fig. 6c**)[77,93], or viral capside-like cages[94,95], a higher and/or more defined enzyme loading can be achieved. In these systems, compartment-to-compartment variations in terms of composition (extrinsic stochastic effects) would be minimal, even though the compartment size is small. An important consideration concerns how substrate molecules can reach the interior of the capsules from the exterior. Recent studies of proteinaceous prokaryotic microcompartments have shown that selective substrate permeability across a lipid-free compartment shell occurs through pore proteins[76,96]. If these pore proteins could be modified to make them selective to specific solutes, it would be possible to combine the intrinsic advantage of proteinaceous capsules created *in vivo* (a high or defined enzyme loading and little stochastic effects) with a selective shell permeability to make efficient nanoreactors for *in vitro* applications. For example, a 27 nm-sized, phosphatase-containing protein capsules in which the substrate permeability across the capsule shell was controlled by the structure of the shell-forming proteins, was reported (**Fig. 6b**)[77]. It has also been shown that 58 nm-sized protein cages

containing three different types of enzymes − at well-defined amounts and ratios – can be prepared through an elegant *in vivo* protein synthesis and assembly approach (**Fig. 6c**)[93] that minimizes stochastic variations, a result difficult to achieve by *in vitro* methods. Such types of protein capsules can also be used for *in vivo* applications, in which compartmentalized enzymatic cascade reactions are designed to operate inside cells[94]. (2141 words)

## 3. Conclusions and perspective

Although the idea of immobilizing enzymes for *in vitro* applications is not new[1,11,97], challenges remain for a *stable*, *efficient* and *spatially controlled localization of active enzymes* participating in *cascade reactions* on surfaces or within compartments. If one claims that a co-localization of enzymes involved in cascade reactions has a better performance than a proper reference system, *convincing* quantitative experimental evidence is required. This is, however, particularly challenging, for example, due to the difficulty in determining the exact amount of confined enzyme, either per surface area or per volume. It may well be that efficient substrate channelling is difficult for *in vitro* enzymatic cascade reactions with enzymes that do not operate together *in vivo*.

Enzymatic fuel cells, devices that transform chemical energy (*e.g.* organic waste) into electrical energy through biochemical transformations, are a promising application for *surface-confined enzymatic cascade reactions*[98]. Here, the development of stable electrode-surface confined sequential multi-step enzymatic reactions is one approach for obtaining desired current and power densities for such devices. To achieve this goal, the preparation of an optimally nanostructured electrode, for example a porous electrically conductive material with a large surface area[56], has to be combined with an optimal enzyme immobilization on this particular material, for example by using DNA as structural scaffold[42,98]. Whether enzymatic fuel cells will ever be available commercially not only depends on the general performance of a device but also on the costs for their fabrication. Therefore, the development of simple, cheap and reproducible enzyme immobilization methods remains an important goal, in addition to the large scale production of cheap and stable enzymes, possibly optimized *via in vitro* evolution approaches[21].

With respect to applications of *volume-confined enzymatic cascade reactions*, vesicular compartments offer unique opportunities *in vitro* as well as *in vivo* as compartmentalized enzymatic nanoreactors. Clearly, artificial vesicles (formed from natural phospholipids or from fully synthetic block copolymers), lipidic bilayer-based organelles and biological cells have obvious structural similarities. One may even think of using polymersomes containing entrapped enzymes as artificial organelles for incorporation into living cells[99-101]. At the moment, it is too early to conclude whether such a futuristic idea will ever lead to successful real applications. Critical research should be devoted to this field. One specific challenge in this respect is the efficient loading of vesicles with enzymes, independent of whether the vesicles are prepared from amphiphilic block copolymers or phospholipids. One possible alternative approach could be the use of protein capsules as enzyme-containing compartment systems, characterized by a high, or well defined, and non-stochastic enzyme entrapment. An immediate need here is to develop methods to control the capsule shell permeability.

With respect to biological cells viewed as highly complex, dynamic, molecularly crowded and evolvable compartment systems[4], in which all chemical transformations are driven by surface- and volume-confined enzymatic reactions, one active and fascinating field of research deals with the synthesis of cell-like model systems in order to study the key principles of biological cells [85,102]. This may also lead to the development of reasonable models of the likely precursors which are thought to have preceded the first cells at the origin of life ( “protocells”)[103].

In general, the majority of the often rather sophisticated systems involving confined enzymes are based on a large number of previous experiments from various extensive basic research studies in seemingly independent fields. This includes, but is not limited to, investigations of (i) the self-assembly and guided assembly of amphiphiles to form vesicles, micelles, reverse micelles or supported bilayers; (ii) the synthesis of fluorescent or fluorogenic molecules and the concomitant improvement of fluorescent detection systems, which enable the investigation of single-enzyme kinetics[104-106] and quantification at low substrate conversion; and (iii) investigations of isolated enzymes with respect to enzyme kinetics and structure analysis. Basic research has created and will continue to create the

ideal foundation for the development of new artificial systems, with important technological implications. (639 words)

## References


1. Grunwald, P. *Biocatalysis: Biochemical Fundamentals and Applications* (Imperial College Press, London, 2009).

2. Purich, D. L. *Enzyme Kinetics: Catalysis & Control* (Elsevier, Amsterdam, 2010).

3. Nagel, Z. D., Klinman, J. P. A 21st century revisionist's view at a turning point in enzymology. *Nature Chem. Biol.* **5**, 543-550 (2009).

4. Ellis, R. J. Macromolecular crowding: Obvious but underappreciated. *Trends Biochem. Sci.* **26**, 597-604 (2001).

5. Alberts, B., Johnson, A., Lewis, J., Morgan, D., Raff, M., Roberts, K., Walter, P. *Molecular Biology of the Cell*, 6th ed. (Garland Science, Taylor & Francis Group, New York, 2015).

6. Conrado, R. J., Varner, J. D., DeLisa, M. P. Engineering the spatial organization of metabolic enzymes : Mimicking nature's synergy. *Curr. Opin. Biotechnol.* **19**, 492-499 (2008).

7. Kunkel, J. Asuri, P. Function, structure, and stability of enzymes confined in agarose gels. *PLOS ONE* **9**, e86785 (2014).

8. Schoffelen, S., van Hest, J. C. M. Chemical approaches for the construction of multi-enzyme reaction systems. *Curr. Opin. Struct. Biol.* **23**, 613-621 (2013).

9. Jia, F., Narasimhan, B., Mallapragada, S. Materials-based strategies for multi-enzyme immobilization and co-localization: A Review. *Biotechnol. Bioeng.* **111**, 209-222 (2013).

10. van Oers, M. C. M., Rutjes, F. P. J. T., van Hest, J. C. M. Cascade reactions in nanoreactors. *Curr. Opin. Biotechnol.* **28**, 10-16 (2014).

11. Mateo, C., Palomo, J. M., Fernandez-Lorente, G., Guisan, J. M., Fernandez-Lafuente, R. Improvement of enzyme activity, stability and selectivity via immobilization techniques. *Enzyme Microb. Technol.* **40,** 1451-1463 (2007).

12. Hanefeld, U., Gardossi, L., Magner, E. Understanding enzyme immobilisation. *Chem. Soc. Rev.* **38**, 453-468 (2009).

13. Zhang, Y.-H. P. Substrate channeling and enzyme complexes for biotechnological applications. *Biotechnol. Adv.* **29**, 715-725 (2011).

14. Sheldon, R. A., van Pelt, S. Enzyme immobilisation in biocatalysis: why, what and how. *Chem. Soc. Rev.* **42**, 6223-6235 (2013).

15. Nelson, C. J., Li, L., Millar, H. A. Quantitative analysis of protein turnover in plants. *Proteomics* **14**, 579-592 (2014).

16. Rodrigues, R. C., Berenguer-Murcia, Á., Fernandez-Lafuente, R. Coupling chemical modification and immobilization to improve the catalytic performance of enzymes. *Adv. Synth. Catal.* **353**, 2216-2238 (2011).

17. Davis, B. G., Boyer, V. Biocatalysis and enzymes in organic synthesis. *Nat. Prod. Rep.* **18**, 618-640 (2001).

18. Kobaysahi, S., Makino, A. Enzymatic polymer synthesis: An opportunity for green polymer chemistry. *Chem. Rev.* **109**, 5288-5353 (2009).

19. Busto, E., Gotor-Fernández, V., Gotor, V. Hydrolases: catalytically promiscuous enzymes for non-conventional reactions in organic synthesis. *Chem. Soc. Rev.* **39**, 4504-4523 (2010).

20. Hollmann, F., Arends, I. W. C. E., Buehler, K., Schallmey, A., Bühler, B. Enzyme-mediated oxidations for the chemist. *Green Chem.* **13**, 226-265 (2011).

21. Reetz, M. F. Biocatalysis in organic chemistry and biotechnology: Past, present, and future*. J. Am. Chem. Soc.* **135**, 12480-12496 (2013).

22. Kazenwadel, F., Franzreb, M., Rapp, B. E. Synthetic enzyme supercomplexes: co-immobilization of enzyme cascades. *Anal. Methods* **7**, 4030-4037 (2015).

23. Agapakis, C. M., Boyle, P. M., Silver, P. A. Natural strategies for the spatial optimization of metabolism in synthetic biology. *Nature Chem. Biol.* **8**, 527-535 (2012).

24. Ghomashchi, F., Yu, B.-Z., Berg, O., Jain, M. K., Gelb, M. H. Interfacial catalysis by phospholipase $A_2$: Substrate specificity in vesicles. *Biochemistry* **30**, 7318-7329 (1991).

25. Sanchez, S. A., Bagatolli, L. A., Gratton, E., Hazlett, T. L. A Two-photon view of an enzyme at work: *Crotalus atrox* venom interaction with single-lipid and mixed-lipid giant unilamellar vesicles. $PLA_2$. *Biophys. J.* **82**, 2232-2243 (2002).

26. Tabaei, S. R., Rabe, M., Zetterberg, H., Zhdanov, V. P., Höök, F. Single Lipid vesicle assay for characterizing single-enzyme kinetics of phospholipid hydrolysis in a complex biological fluid. *J. Am. Chem. Soc.* **135**, 14151-14158 (2013).

27. Martinek, K., Levashov, A. V., Klyachko, N. L., Khmelnistki, Y. L., Berezin, I. V. Micellar enzymology. *Eur. J. Biochem.* **155**, 453-468 (1986).

28. Luisi, P. L., Giomini, M., Pileni, M. P., Robinson, B. H. Reverse micelles as hosts for proteins and small molecules. *Biochim. Biophys. Acta* **947**, 209-246 (1988).

29. Carvalho, C. M. L., Cabral, J. M. S. Reverse micelles as reaction media for lipases. *Biochimie* **82**, 1063-1085 (2000).

30. Grandbois, M., Clausen-Schaumann, H., Gaub, H. Atomic force microscope imaging of phospholipid bilayer degradation by phospholipase $A_2$. *Biophys. J.* **74**, 2398-2404 (1998).

31. Dutta, D., Pulsipher, A., Yousaf, M. N. PI3 kinase enzymology on fluid lipid bilayers. *Analyst* **139**, 5127-5133 (2014).

32. Fornera, S., Kuhn, P., Lombardi, D., Schlüter, A. D., Dittrich, P. S., Walde, P. Sequential immobilization of enzymes in microfluidic channels for cascade reactions. *ChemPlusChem* **77**, 98-101 (2012).

33. Küchler, A., Bleich, J. N., Sebastian, B., Dittrich, P. S., Walde, P. Stable and simple immobilization of proteinase K inside glass tubes and microfluidic channels. *ACS Appl. Mater. Interfaces* **7,** 25970-25980 (2015).

34. Yu, J., Zhang, Y., Liu, S. Enzymatic reactivity of glucose oxidase confined in nanochannels. *Biosens. Bioelectron.* **55**, 307-312 (2014).

35. Johnson, B. J., Algar, W. R., Malanoski, A. P., Ancona, M. G., Medintz, I. L. Understanding enzymatic acceleration at nanoparticle interfaces: Approaches and challenges. *Nano Today* **9**, 102-131 (2014).

36. Vashist, S. K., Lam, E., Hrapovic, S., Male, K. B., Luong, J. H. T. Immobilization of antibodies and enzymes on 3‑aminopropyltriethoxysilane-functionalized bioanalytical platforms for biosensors and diagnostics. *Chem. Rev.* **114**, 11083-11130 (2014).

37. Palazzo, G., Colafemmina, G., Guzzoni Iudice, C., Mallardi, A. Three immobilized enzymes acting in series in layer by layer assemblies: Exploiting the trehalase-glucose oxidase-horseradish peroxidase cascade reactions for the optical determination of trehalose. *Sensors and Actuators B* **202**, 217-223 (2014).

38. Fornera, S., Bauer, T., Schlüter, A. D., Walde, P. Simple enzyme immobilization inside glass tubes for enzymatic cascade reactions. *J. Mater. Chem.* **22**, 502-511 (2012).

39. Küchler, A., Adamcik, J., Mezzenga, R., Schlüter, A. D., Walde, P. Enzyme immobilization on silicate glass through simple adsorption of dendronized polymer-enzyme conjugates for localized enzymatic cascade reactions, *RSC Adv.* **5**, 44530-44544 (2015).

40. Linko, V., Eerikäinen, M., Kostiainen, M. A. A modular DNA origami-based enzyme cascade nanoreactor. *Chem. Commun.* **51**, 5351-5354 (2015).

41. Castellana, M., Wilson, M. Z., Xu, Y., Joshi, P., Cristea, I. M., Rabinowitz, J. D., Gitai, Z., Wingreen, N. S. Enzyme clustering accelerates processing of intermediates through metabolic channeling. *Nature Biotechnol.* **32**, 1011-1018 (2014).

42. Fu, J., Liu, M., Liu, Y., Woodbury, N. W., Yan, H. Interenzyme substrate diffusion for an enzyme cascade organized on spatially addressable DNA nanostructures. *J. Am. Chem. Soc.* **134**, 5516-5519 (2012).

43. Wu, F., Minteer, S. Krebs Cycle Metabolon: Structural evidence of substrate channeling revealed by cross-linking and mass spectrometry. *Angew. Chem. Int. Ed.* **54**, 1851-1854 (2015).

527 44. Dueber, J. E., Wu, G. C., Malmirchegini, G. R., Moon, T. S., Petzold, C. J., Ullal, A. V.,
528 Prather, K. L. J., Keasling, J. D. Synthetic protein scaffolds provide modular control over
529 metabolic flux, *Nature Biotechnol.* **27**, 753-759 (2009).

530 45. Gustafsson, H., Küchler, A., Holmberg, K., Walde, P. Co-immobilization of enzymes with
531 the help of a dendronized polymer and mesoporous silica nanoparticles. *J. Mater. Chem. B* **3**,
532 6174-6184 (2015).

533 46. Kang, W., Liu, J., Wang, J., Nie, Y., Guo, Z., Xia, J. Cascade biocatalysis by
534 multienzyme−nanoparticle assemblies. *Bioconjugate Chem.* **25**, 1387-1394 (2014).

535 47. You, C.-C., Agasti, S. S., De, M., Knapp, M. J., Rotello, V. M. Modulation of the catalytic
536 behavior of α-chymotrypsin at monolayer-protected nanoparticle surfaces. *J. Am. Chem. Soc.*
537 **128**, 14612-14618 (2006).

538 48. Kim, J., Jia, H., Wang, P. Challenges in biocatalysis for enzyme-based biofuel cells.
539 *Biotechnol. Adv.* **24** 296-308 (2006).

540 49. Willner, I., Yan, Y.-M., Willner, B., Tel-Vered, R. Integrated enzyme-based biofuel cells – A
541 review. *Fuel Cells* **9**, 7-24 (2009).

542 50. Osman, M. H., Shah, A. A., Walsh, F. C. Recent progress and continuing challenges in bio-
543 fuel cells. Part I: Enzymatic cells. *Biosens. Bioelectron.* **26**, 3087-3102 (2011).

544 51. Leech, D., Kavanagh, P., Schuhmann, W. Enzymatic fuel cells: Recent progress.
545 *Electrochim. Acta* **84** 223-234 (2012).

546 52. Kim, Y. H., Campbell, E., Yu, J., Minteer, S. D., Banta, S. Complete oxidation of methanol
547 in biobattery devices using a hydrogel created from three modified dehydrogenases. *Angew.*
548 *Chem.* **125**, 1477-1480 (2013).

549 53. de Poulpiquet, A., Ciaccafava, A., Lojou, A. New trends in enzyme immobilization at
550 nanostructured interfaces for efficient electrocatalysis in biofuel cells. *Electrochim. Acta* **126,**
551 104-114 (2014).

552 54. Luz, R. A. S., Pereira, A. R., de Souza, J. C. P., Sales, F. C. P. F., Crespilho, F. N. Enzyme
553 biofuel cells: Thermodynamics, kinetics and challenges in applicability. *ChemElectroChem* **1**,
554 1751-1777 (2014).

555 55. Heller, A., Feldman, B. Electrochemical glucose sensors and their applications in diabetes
556 management. *Chem. Rev.* **108**, 2482-2505 (2008).

557 56. Tsujimura, S., Murata, K., Akatsuka, W. Exceptionally high glucose current on a
558 hierarchically structured porous carbon electrode with "wired" flavin adenine dinucleotide-
559 dependent glucose dehydrogenase. *J. Am. Chem. Soc.* **136**, 14432-14437 (2014).

560 57. Ohara, T. J., Rajagopalan, R., Heller, A. Glucose electrodes based on cross-linked
561 $[Os(bpy)2Cl]^{+/2+}$ complexed poly(1-vinylimidazole) films. *Anal. Chem.* **65**, 3512-3517 (1993).

562 58. Junker, K., Zandomeneghi, G., Guo, Z., Kissner, R., Ishikawa, T., Kohlbrecher, J., Walde, P.
563 Mechanistic aspects of the horseradish peroxidase-catalysed polymerisation of aniline in the
564 presence of AOT vesicles as templates. *RSC Adv.* **2**, 6478-6495 (2012).

565 59. Walde, P., Umakoshi, H., Stano, P., Mavelli, F. Emergent properties arising from the
566 assembly of amphiphiles. Artificial vesicle membranes as reaction promoters and regulators.
567 *Chem. Commun.* **50**, 10177-10197 (2014).

568 60. Chen, A. H., Silver, P. A. Designing biological compartmentalization. *Trends Cell Biol.* **22**,
569 662-670 (2012).

570 61. Satori, C. P., Henderson, M. M., Krautkramer, E. A., Kostal, V., Distefano, M. M., Arriaga,
571 E. A. Bioanalysis of eukaryotic organelles. *Chem. Rev.* **113**, 2733-2811 (2013).

572 62. Chowdhury C., Sinha, S., Chun, S., Yeates, T. O., Bobik, T. A. Diverse bacterial
573 microcompartment organelles. *Microbiol. Mol. Biol. Rev.* **78**, 438-468 (2014).

574 63. Yeates T. O., Kerfeld, C. A., Heinhorst, S., Cannon, G. C., Shively, J. M. Protein-based
575 organelles in bacteria: carboxysomes and related microcompartments. *Nature Rev.*
576 *Microbiol.* **6**, 681-691 (2008).

577 64. Lee, H., DeLoache, W. C., Dueber, J. E. Spatial organization of enzymes for metabolic
578 engineering. *Metabol. Eng.* **14**, 242–251 (2012).

579 65. Cannon, G. C., Heinhorst, S., Kerfeld, C. A. Carboxysomal carbonic anhydrases: Structure
580 and role in microbial $CO_2$ fixation. *Biochim. Biophys. Acta* **1804**, 382-392 (2010).

66. Kerfeld, C. A., Heinhorst, S., Cannon, G. C. Bacterial microcompartments. *Annu. Rev. Microbiol.* **64**, 391-408 (2010).

67. Heinhorst, S., Williams, E. B., Cai, F., Murin, C. D., Shively, J. M., Cannon, G. C. Characterization of the carboxysomal carbonic anhydrase CsoSCA from *Halothiobacillus neapolitanus*. *J. Bacteriol.* **188**, 8087-8094 (2006).

68. Walde, P., Ichikawa, S. Enzymes inside lipid vesicles: preparation, reactivity and applications. *Biomol. Eng.* **18**, 143-177 (2001).

69. Walde, P., Cosentino, K., Engel, H., Stano, P. Giant vesicles: Preparations and applications. *ChemBioChem* **11**, 848-865 (2010).

70. Theberge, A. B., Courtois, F., Schaerli, Y., Fischlechner, M., Abell, C., Hollfelder, F., Huck, W. T. S. Microdroplets in microfluidics: An evolving platform for discoveries in chemistry and biology. *Angew. Chem. Int. Ed.* **49**, 5846-5868 (2010).

71. Christensen, S. M., Bolinger, P.-Y., Hatzakis, N. S., Mortensen, M. W., Stamou, D. Mixing subattolitre volumes in a quantitative and highly parallel manner with soft matter nanofluidics. *Nature Nanotechnol.* **7**, 51-55 (2012).

72. Miyake, Y. Enzymatic reaction in water-in-oil microemulsions. *Colloids Surf. A: Physicochem. Eng. Asp.* **109**, 255-262 (1996).

73. Ruckenstein, E., Karpe, P. Enzymatic super- and subactivity in nonionic reverse micelles. *J. Phys. Chem.* **95**, 4869-4882 (1991).

74. Walde, P., Marzetta, B. Bilayer Permeability-based substrate selectivity of an enzyme in liposomes. *Biotechnol. Bioeng.* **57**, 216-219 (1998).

75. Yoshimoto, M., Okamoto, M., Ujihashi, K., Okita, T. Selective oxidation of D‑amino acids catalyzed by oligolamellar liposomes intercalated with D‑amino acid oxidase. *Langmuir* **30**, 6180-6186 (2014).

76. Chowdhury, C., Chun, S., Pang, A., Sawaya, M. R., Sinha, S., Yeates, T. O., Bobik, T. A. Selective molecular transport through the protein shell of a bacterial microcompartment organelle. *Proc. Natl. Acad. Sci. USA* **112**, 2990-2995 (2015).

77. Glasgow, J. E., Asensio, M. A., Jakobson, C. M., Francis, M. B., Tullman-Ercek, D. Influence of electrostatics on small molecule flux through a protein nanoreactor. *ACS Synth. Biol.* **4**, 1011-1019 (2015).

78. Weitz, M., Kim, J., Kapsner, K., Winfree, E., Franco, E., Simmel, F. C. Diversity in the dynamical behaviour of a compartmentalized programmable biochemical oscillator. *Nature Chem.* **6**, 295-302 (2014).

79. Karig, D. K., Jung, S.-Y., Srijanto, B., Collier, C. P., Simpson, M. L. Probing cell-free gene expression noise in femtoliter volumes. *ACS Synth. Biol.* **2**, 497-505 (2013).

80. Sintra, T. E., Ventura, S. P. M., Coutinho, J. A. P. Superactivity induced by micellar systems as the key for boosting the yield of enzymatic reactions. *J. Mol. Catal. B: Enzymatic* **107**, 140-151 (2014).

81. Moyano, F., Falcone, R. D., Mejuto, J. C., Silber, J. J., Correa, N. M. Cationic reverse micelles create water with super hydrogen-bond-donor capacity for enzymatic catalysis: Hydrolysis of 2-naphthyl acetate by α-chymotrypsin. *Chem. Eur. J.* **16**, 8887-8893 (2010).

82. Biswas, R., Das, A. R., Pradhan, T., Touraud, D., Kunz, W., Mahiuddin, S. Spectroscopic studies of catanionic reverse microemulsion: Correlation with the superactivity of horseradish peroxidase enzyme in a restricted environment *J. Phys. Chem. B* **112**, 6620-6628 (2008).

83. Moniruzzaman, M., Kamiya, N., Goto, M. Biocatalysis in water-in-ionic liquid microemulsions: A case study with horseradish peroxidase. *Langmuir* **25**, 977-982 (2009).

84. Pereira de Souza, T., Stano, P., Luisi, P. L. The minimal size of liposome-based model cells brings about a remarkably enhanced entrapment and protein synthesis. *ChemBioChem* **10**, 1056-1063 (2009).

85. Nourian, Z., Roelofsen, W., Danelon, C. Triggered gene expression in fed-vesicle microreactors with a multifunctional membrane. *Angew. Chem. Int. Ed.* **51**, 3114-3118 (2012).

86. Nishimura, K., Tsuru, S., Suzuki, H., Yomo, T. Stochasticity in gene expression in a cell-sized compartment. *ACS Synth. Biol.* **4**, 566-576 (2015).

636 87. Mavelli F., Stano P. Experiments and numerical modelling on the capture and
637 concentration of transcription-translation machinery inside vesicles. *Artificial Life* **21**, 1-19
638 (2015).

639 88. Petrovics, I., Hong, K., Omburo, G., Hu, Q. Z., McGuinn, W. D., Sylvester, D., Tamulinas, C.,
640 Papahadjopoulos, D., Jaszberenyi, J. C., Barcza, T., Way, J. L. Antagonism of paraoxon
641 intoxication by recombinant phosphotriesterase encapsulated within sterically stabilized
642 liposomes. *Toxicol. Appl. Pharmacol.* **156**, 56-63 (1999).

643 89. Torchilin, V. Recent advances with liposomes as pharmaceutical carriers. *Nature Rev.*
644 *Drug. Discov.* **4**, 145-160 (2005).

645 90. Yoshimoto, M., Wang, S., Fukunaga, K., Fournier, D., Walde, P., Kuboi, R., Nakao, K. Novel
646 immobilized liposomal glucose oxidase system using the channel protein OmpF and catalase.
647 *Biotechnol. Bioeng.* **90**, 231-238 (2005).

648 91. Peters, R. J. R. W., Marguet, M., Marais, S., Fraaije, M. W., van Hest, J. C. M.,
649 Lecommandoux, S. Cascade reactions in multicompartmentalized polymersomes. *Angew.*
650 *Chem. Int. Ed.* **53**, 146-150 (2014).

651 92. Louzao, I., van Hest, J. C. M. Permeability effects on the efficiency of antioxidant
652 nanoreactors. *Biomacromolecules* **14**, 2364-2372 (2013).

653 93. Patterson, D. P., Schwarz, B., Waters, R. S., Gedeon, T., Douglas, T. Encapsulation of an
654 enzyme cascade within the bacteriophage P22 virus-like particle. *ACS Chem. Biol.* **9**, 359-365
655 (2014).

656 94. Chen, R., Chen, Q., Kim, H., Siu, K.-H., Sun, Q., Tsai, S.-L., Chen, W. Biomolecular scaffolds
657 for enhanced signaling and catalytic efficiency. *Curr. Opin. Biotechnol.* **28**, 59-68 (2014).

658 95. Patterson, D. P., Prevelige, P. E., Douglas, T. Nanoreactors by programmed enzyme
659 encapsulation inside the capsid of the bacteriophage P22. *ACS Nano* **6**, 5000-5009 (2012).

660 96. Bobik, T. A., Lehman, B. P., Yeates, T. O. Bacterial microcompartments: widespread
661 prokaryotic organelles for isolation and optimization of metabolic pathways. *Mol. Microbiol.*
662 **98**, 193-207 (2015).

663 97. Ariga, K., Ji, Q., Mori, T., Naito, M., Yamauchi, Y., Abe, H., Hill, J. P. Enzyme
664 nanoarchitectonics: organization and device application. *Chem. Soc. Rev.* **42**, 6322-6345
665 (2013).

666 98. Rasmussen, M., Abdellaoui, S., Minteer, S. D. Enzymatic biofuel cells: 30 years of critical
667 advancements. *Biosens. Bioelectron.* **76**, 91-102 (2016).

668 99. Marguet, M., Bonduelle, C., Lecommandoux, S. Multicompartmentalized polymeric
669 systems: towards biomimetic cellular structure and function. *Chem. Soc. Rev.* **42**, 512-529
670 (2013).

671 100. Tanner, P., Balasubramanian, V., Palivan, C. G. Aiding nature's organelles: Artificial
672 peroxisomes play their role. *Nano Lett.* **13**, 2875-2883 (2013).

673 101. Kim, E. Y., Tullman-Ercek, D. Engineering nanoscale protein compartments for synthetic
674 organelles. *Curr. Opin. Biotechnol.* **24**, 627-632 (2013).

675 102. Hansen, M. M. K., Meijer, L. H. H., Spruijt, E., Maas, R. J. M., Ventosa Rosquelles, M.,
676 Groen, J., Heus, H. A., Huck, W. T. S. Macromolecular crowding creates heterogeneous
677 environments of gene expression in picoliter droplets. *Nature Nanotechnol.* **11**, 191-197
678 (2016).

679 103. Stano, P., Luisi, P. L. Achievements and open questions in the self-reproduction of
680 vesicles and synthetic minimal cells. *Chem. Commun.* **46**, 3639-3653 (2010).

681 104. Ishitsuka, Y., Okumus, B., Arslan, S., Chen K. H., Ha, T. Temperature-independent porous
682 nanocontainers for single-molecule fluorescence studies. *Anal. Chem.* **82**, 9694-9701 (2010).

683 105. Christensen, A. L., Lohr, C., Christensen, S. M., Stamou, D. Single vesicle biochips for
684 ultra-miniaturized nanoscale fluidics and single molecule bioscience. *Lab Chip* **13**, 3613-3625
685 (2013).

686 106. Piwonski, H. M., Goomanovsky, M., Bensimon, D., Horovitz, A., Haran, G. Allosteric
687 inhibition of individual enzyme molecules trapped in lipid vesicles. *Proc. Natl. Acad. Sci. USA*
688 **109**, E1437-E1443 (2012).

689 107. Pavlidis, I. V., Patila, M., Bornscheuer, U. T., Gournis, D., Stamatis, H. Graphene-based
690 nanobiocatalytic systems: recent advances and future prospects. *Trends Biotechnol.* **32**, 312-
691 320 (2014).

692 108. Fang, W., Ji, P. Enzymes immobilized on carbon nanotubes. *Biotechnol. Adv.* **29**, 889-895
693 (2011).

694 109. Magner, E. Immobilisation of enzymes on mesoporous silicate materials. *Chem. Soc.*
695 *Rev.*, **42**, 6213-6266 (2013).

696 110. Nandiyanto, A. B. D., Kim, S.-G., Iskandar, F., Okuyama, K. Synthesis of spherical
697 mesoporous silica nanoparticles with nanometer-size controllable pores and outer
698 diameters. *Micropor. Mesopor. Mater.* **120**, 447-453 (2009).

699 111. Jia, H., Zhu, G., Wang, P. Catalytic behaviors of enzymes attached to nanoparticles: The
700 effect of particle mobility. *Biotechnol. Bioeng.* **84**, 406-414 (2003).

701 112. Yoshimoto, M., Sakamoto, H., Shirakami, H. Covalent conjugation of tetrameric bovine
702 liver catalase to liposome membranes for stabilization of the enzyme tertiary and quaternary
703 structures. *Colloids Surf. B: Biointerfaces* **69**, 281-287 (2009).

704 113. Huang, X., Li, M., Mann, S. Membrane-mediated cascade reactions by enzyme–polymer
705 proteinosomes. *Chem. Commun.* **50**, 6278-6280 (2014).

706 114. Park, M., Qing Sun, Q., Liu, F., DeLisa, M., Chen, W. Positional assembly of enzymes on
707 bacterial outer membrane vesicles for cascade reactions. *PLoS ONE* **9**(5): e97103 (2014).

708 115. Liu, F., Banta, S., Chen, W. Functional assembly of a multi-enzyme methanol oxidation
709 cascade on a surface-displayed trifunctional scaffold for enhanced NADH production. *Chem.*
710 *Commun.* **49**, 3766-3768 (2013).

711 116. Meredith, M. T., Minteer, S. D. Biofuel cells: Enhanced enzymatic bioelectrocatalysis.
712 *Annu. Rev. Anal. Chem.* **5**, 157-179 (2012).

713 117. Leech, D., Kavanagh, P., Schuhmann, W. Enzymatic fuel cells: Recent progress.
714 *Electrochim. Acta* **84**, 223-234 (2012).

715 118. Orlich, B., Schomäcker, R. Enzyme catalysis in reverse micelles. *Adv. Biochem. Eng.*
716 *Biotechnol.* **75**, 185-208 (2002).

717 119. Liu, Y., Jung, S.-Y., Collier, C. P. Shear-driven redistribution of surfactant affects enzyme
718 activity in well-mixed femtoliter droplets. *Anal. Chem.* **81**, 4922-4928 (2009).

719 120. Nardin, C., Widmer, J., Winterhalter, M., Meier, W. Amphiphilic block copolymer
720 nanocontainers as bioreactors. *Eur. Phys. J. E* **4**, 403-410 (2001).

721 121. Chen, Q., Schönherr, H., Vancso, G. J. Block-copolymer vesicles as nanoreactors for
722 enzymatic reactions. *Small* **5**, 1436-1445 (2009).

723 122. Vriezema, D. M., Garcia, P. M. L., Sancho Oltra, N., Hatzakis, N. S., Kuiper, S. M., Nolte,
724 R. J. M., Rowan, A. E., van Hest, J. C. M. Positional assembly of enzymes in polymersome
725 nanoreactors for cascade reactions. *Angew. Chem.* **119**, 7522-7526 (2007).

726 123. Hansen, J. S., Elbing, K., Thompson, J. R., Malmstadt, N., Lindkvist-Petersson, K. Glucose
727 transport machinery reconstituted in cell models. *Chem. Commun.* **51**, 2316-1319 (2015).

728 124. Comellas-Aragonès, M., Engelkamp, H., Claessen, V. I., Sommerdijk, N. A. J. M., Rowan,
729 A. E., Christianen, P. C. M., Maan, J. C., Verdun, B. J. M., Cornelissen, J. J. L. M., Nolte, R. J. M.
730 A virus-based single-enzyme nanoreactor. *Nature Nanotechnol.* **2**, 635-639 (2007).

731 125. Price, A. D., Zelikin, A. N., Wang, Y., Caruso, F. Triggered enzymatic degradation of DNA
732 within selectively permeable polymer capsule microreactors. *Angew. Chem. Int. Ed.* **48**, 329-
733 332 (2009).

734 126. Kreft, O., Prevot, M., Möhwald, H., Sukhorukov, G. B. Shell-in-shell microcapsules: A
735 novel tool for integrated, spatially confined enzymatic reactions. *Angew. Chem. Int. Ed.* **46**,
736 5605-5608 (2007).

737 127. Sakr, O. S., Borchard, G. Encapsulation of enzymes in layer-by-layer (LbL) structures:
738 Latest advances and applications. *Biomacromolecules* **14**, 2117-2135 (2013).

739 128. Hosta-Rigau, L., York-Duran, M. J., Zhang, Y., Goldie, K. N., Städler, B. Confined multiple
740 enzymatic (cascade) reactions within poly(dopamine)-based capsosomes. *ACS Appl. Mater.*
741 *Interfaces* **6**, 12771-12779 (2014).

129. Gorris, H. H., Walt, D. R. Mechanistic aspects of horseradish peroxidase elucidated through single-molecule studies. *J. Am. Chem. Soc.* **131**, 6277-6282 (2009).

130. Liebherr, R. B., Gorris, H. H. Enzyme molecules in solitary confinement. *Molecules* **19**, 14417-14445 (2014).

**Acknowledgement**

Financial support for the stimulating meetings of the COST action CM1304 on the "Emergence and Evolution of Complex Chemical systems" is highly appreciated.

**Additional Information**

Correspondence and requests for materials should be addressed to P.W.

**Competing financial interests**

The authors declare no competing financial interests.

**Fig. 1:**

**Some of the different possibilities of immobilizing enzymes on solid supports for surface-confined enzymatic reactions in an aqueous environment.** The green and dark purple objects represent two different types of enzymes with their active sites indicated as indentations. For enzymatic cascade reactions to occur efficiently, immobilization of the different enzymes involved should occur in a defined way by placing them at specific positions and relative ratio. The enzymes' activity must be retained, and the system must have acceptable storage and operational stabilities. Different strategies have been developed to immobilize enzymes on solid supports: **a,** by direct enzyme adsorption *via* non-covalent interactions between the enzymes and the support[36]; **b,** *via* one or more organic linker molecules which allows for covalent bonding between the support and the enzymes[36] and which ensures that the enzyme is kept at a distance from the surface; **c,** *via* adsorbed or covalently bound self-assembled monolayers; **d,** *via* adsorbed or covalently bound bilayers of amphilphiles; **e**, *via* non-covalently adsorbed organic polymers[32,38] or proteins (the red object in **e** denotes the protein avidin (or streptavidin or neutravidin) with its four biotin-binding sites)[36]; or **f,** *via* non-covalently adsorbed dendronized polymer-enzyme conjugates[33,39]. The solid support can be inorganic and smooth (planar silicate glass[33,38,39], dispersed graphene oxides[107] or carbon nanotubes[108]); inorganic and rough (mesoporous silicates[109,110]); or organic (polystyrene particles[111], "DNA origami tiles"[42], vesicles[58,112-114] or cells[115]).

**Fig. 2:**

**Examples of surface-confined enzymatic cascade reactions**. **a,** Localization of biotinylated GOD (= GOx) and HRP by using tubular DNA origami building blocks and neutravidin (NTV). A catalytically active "Dimer-Nanoreactor" containing the two enzymes was obtained, as determined by analyzing the transformation of D-glucose and 3,3',5,5'-tetramethylbenzidine (TMB) at pH = 5.0 in the presence of $O_2$ into TMB imine (TMB*). In the "Reference" measurements, NTV was omitted which decreased the amount of bound enzymes[40]. **b,** Localization of GOD (yellow ) and HRP (purple) at defined distance on the surface of DNA origami tiles. An increased catalytic activity was observed if the inter-enzyme distance was 10 nm, as analyzed with D-glucose and $ABTS^{2-}$ (= 2,2'-Azinobis(3-ethylbenzothiazoline-6-sulfonate)) and $O_2$ as substrates at pH = 7.2. No enhanced activity was found if the inter-enzyme distance was 65 nm, while at a distance of 20 nm, the increase in activity was only small[42]. **c,** Localization of GOD (orange) and HRP (green) on silicate surfaces with the help of a dendronized polymer (blue) and mesoporous silica nanoparticles (grey). GOD was positioned inside the pores of the particles and HRP spatially separated on the particles through covalently linking HRP along the polymer chain, followed by simple adsorption of the obtained polymer-enzyme conjugate. The enzymes remained active for at least 18 days if stored at 4 °C, as analyzed with D-glucose, *o*-phenylenediamine and $O_2$ as substrates (expressed as GOD activity of the cascade reaction, *i.e.,* as determined without admixture of HRP)[45]. **d,** Localization of the three enzymes MenF, MenD and MenH of the menaquinone biosynthetic pathway on CdSe-ZnS core/shell quantum dots. About 16-20 enzyme molecules were bound to each particle. The reaction was more efficient when each particle contained a mixture of the three enzymes than when each particle contained only one type of enzyme. The activity was highest if MemF was in excess over the other two enzymes (case 3), as determined with chorismate as substrate at pH = 7.0 to yield 2-succinyl-6-hydroxy-2,4-cyclohexadiene-1-carboxylate (SHCHC) as product[46]. Figures adapted with minor modifications from: **a**, ref. 40, Royal Society of Chemistry; **b**, ref. 42, American Chemical Society; **c**, ref. 45, Royal Society of Chemistry; **d**, ref. 46, American Chemical Society.

**Fig. 3:**

**Two examples of the application of surface-confined enzymatic reactions**. **a,** Enzymatic fuel cell. Left: Illustration of a membraneless enzymatic fuel cell[116,117] in which the fuel is oxidized at the anode by an immobilized oxidative enzyme (green). The electrons released during the oxidation move through the external wire ($e^-$-flow) to the cathode at which $O_2$ is reduced by the immobilized reductive enzyme (blue). Right: A specific example of an anode which was coated with mesoporous carbon (average pore diameter of 38 nm and a surface roughness of several tens of micrometers) to which the enzyme d-FAD-DGH (= degylcosylated flavin adenine dinucleotide-dependent glucose dehydrogenase, green) was immobilized within a hydrogel formed from poly(1-vinyl-imidazole) which was crosslinked with PEGDGE (= poly(ethylene glycol) diglycidyl ether) and complexed to $[Os(2,2'\text{-bipyridine})_2Cl]^{+/2+}$ for efficient electron transfer. D-glucose was used as fuel, yielding glucono-δ-lactone (oxidized fuel)[56]. **b,** Enzymatic polymerization of aniline on the surface of anionic vesicles catalysed by a redox enzyme which is localised on the vesicle membrane surface[58]. Unilamellar vesicles with a diameter of about 100 nm were prepared from AOT (sodium bis(2-ethylhexyl)sulfosuccinate) in an aqueous salt solution of pH = 4.3. After HRP and the aniline monomers (mainly present as anilinium cation) had associated with the vesicle surface, the aniline oxidation was triggered by adding $H_2O_2$. Polymerization of the obtained aniline radial cation into the emeraldine salt form of polyaniline (PANI-ES) occurred on the vesicle surface. PANI-ES did not form in the absence of the vesicles.

**Fig. 4:**

**Some of the different approaches for volume-confined enzymatic reactions**. **a,** Reverse (or inverted) micellar solutions or w/o microemulsions[27-29,80,118], *i.e.* submicrometer-sized aqueous droplets which are stabilized in a water-immiscible organic solvent – or an ionic liquid[83] – with the help of amphiphilic molecules (surfactants). In the case of reverse micelles, one type of amphiphile stabilizes the water droplets, while for w/o microemulsions, a cosurfactant (often a long chain alcohol) is also used. Typical sizes of the internal aqueous volumes range from 5 nm ($6.5 \cdot 10^{-23}$ L = 65 yL) to 30 nm ($1.4 \cdot 10^{-20}$ L = 14 zL), including the space occupied by the enzymes. For enzymatic cascade reactions with different types of enzymes, different enzyme-containing micellar solutions have to be used. **b,** Micrometer-sized aqueous droplets which are dispersed in a water-immiscible solvent with the help of a shell of amphiphilic molecules which form the boundary layer.[70,119] Water-soluble enzymes are localized in the aqueous volume, which is separated from the bulk organic solvent. Typical droplet sizes vary between 2 µm ($4.2 \cdot 10^{-15}$ L = 4.2 fL) and 20 µm ($4.2 \cdot 10^{-12}$ L = 4.2 pL), usually prepared by microfluidic devices to achieve monodispersity in droplet size[70]. For enzymatic cascade reaction in which different types of enzymes are involved, each water droplet contains the different enzymes in the desired amounts. **c,** Spherical artificial vesicles (called lipid vesicles[68] or liposomes if prepared from biological bilayer-forming amphiphilic phospholipids; or polymeric vesicles (polymersomes),[120-122] if prepared from amphiphilic block copolymers. The internal size of spherical vesicles (D) may vary between about 30 nm (small, $1.4 \cdot 10^{-20}$ L = 14 zL), 100 nm (large, $5.2 \cdot 10^{-19}$ L = 0.52 aL), to several hundred µm (giant, $1.4 \cdot 10^{-6}$ L = 1.4 µL, for D = 300 µm), depending on the method of preparation[68,69]. Although efficient loading of vesicles with water-soluble enzymes may be a challenge[68], once entrapped, the enzymes remain inside the vesicle's aqueous volume due to their macromolecular sizes, separated from the bulk aqueous medium by one or several lamellae of amphiphilic molecules. The schematic drawing shows a unilamellar vesicle with a single lamella. The vesicle shells may be permeable for water and other small, neutral molecules, depending on the physical state of the membrane (temperature dependent packing density). The permeability of the vesicle shells can be modified by varying the chemical structure of the amphiphiles, by using mixtures of amphiphiles, or by inserting pore- or channel-forming peptides and proteins[90,120,123]. For enzymatic cascade reactions involving different types of enzymes, it would be important to co-entrap different types of enzymes inside the same

vesicles with the desired amounts and concentration ratio. **d,** Protein cages, submicrometer-sized compartments (40 – 80 nm) with a boundary which is composed of proteins[77,93,95,124], like virus capsides or prokaryotic microcompartments[62-64,96]. Here, efficient entrapment of enzymes inside protein cages is yet to be achieved, unless the enzyme is part of the inner surface of the shell. The permeability of the shell is determined by the shell structure. **e,** Polymer capsules[125-128] obtained by a layer-by-layer deposition method involving polyelectrolytes and a core structure template which is dissolved and removed after capsule formation[126,128]. The typical size range is 4-10 µm. The layer permeability depends on the polyelectrolyte used and the details of the layer structure. **f,** Arrays of small reaction vessels obtained through chemical etching of glass fibers (vessel diameters between 3 and 10 µm and depths between 0.2 and 5 µm)[129,130]. There is no exchange of matter between the individual, physically separated reaction vessels. The green and dark purple objects represent two different types of enzymes with their active sites indicated as indentations. The pink object in **c** denotes a channel-forming peptide or protein, the orange objects in **d** are capsule shell-forming proteins and the black chains in **e** represent polyelectrolytes. Aqueous solutions are marked in light blue, organic solutions (or ionic liquids) in **a,** which do not mix with water, are marked in light yellow.

**Fig. 5**:

**Two examples of enzymatic reactions inside vesicles**. **a,** Phospholipid-based vesicles containing an encapsulated enzyme for possible *in vivo* applications as detoxifying nanoreactors that circulate in the blood stream[88].Unilamellar vesicles with a diameter of about 100 nm were prepared from a mixture of POPC (1-palmitoyl-2-oleoyl-*sn*-glycero-3-phosphocholine), the pegylated phospholipid PEG-PE (1,2-dipalmitoyl-*sn*-glycero-3-phosphoethanolamine-*N*-[poly(ethylene glycol)-2000], and cholesterol. Cholesterol was included for increasing the stability of the vesicles; PEG served as steric stabilizer for preventing rapid clearance by the immune system after intravenous injection. The vesicles contained in their aqueous interior a phosphotriesterase which catalysed the hydrolysis of paraoxon (a metabolite of parathion which is used as insecticide) into diethylphosphate and *p*-nitrophenol. Paraoxon is expected to translocate from the bulk medium into the vesicles' interior since paraoxon is partially hydrophobic and a relative small molecule. **b,** Immobilized phospholipid-based vesicles containing two encapsulated enzymes for *in vitro* applications as enzymatic nanoreactors for the oxidation of D-glucose[90].Unilamellar vesicles with a diameter of about 100 nm were prepared from a mixture of phosphatidylcholines from egg yolk (egg PC), DMPE (1,2-dimyristoyl-*sn*-glycero-3-phosphoethanolamine), and cholesterol. The vesicles contained the two enzymes GOD and catalase and were immobilized on chitosan beads *via* glutaraldehyde linker molecules. The entrapped GOD catalysed the oxidation of D-glucose to glucono-δ-lactone and $H_2O_2$; $H_2O_2$ disproportionation to $O_2$ and $H_2O$ was catalysed by the co-entrapped catalase. The transport of D-glucose from the bulk medium into the vesicles' interior was facilitated by the incorporation of the channel-forming protein OmpF into the membrane.

**Fig. 6:**

**Examples of volume-confined enzymatic reactions**. **a,** Polymersome-confined enzymatic cascade reaction for the elimination of superoxide radical anions ($O_2^{\bullet -}$) inside the polymersomes by co-entrapped Cu/Zn superoxide dismutase (SOD1) and catalase (CAT)[92]. Top: Schematic drawing of one single polymersome encapsulating SOD1 and CAT which cooperatively catalyze the conversion of $O_2^{\bullet -}$ into dioxygen and water. The superoxide anions, as well as $O_2$ and $H_2O$ permeate the polymersome membrane. The polymersome membranes were composed of either poly(styrene)$_{40}$-*b*-poly-(L-isocyanoalanine(2-thiophen-3-yl-ethyl)amide)$_{50}$ (PS-PIAT), or poly(styrene)$_{160}$-*b*-poly(ethylene glycol)$_{24}$ (PS-PEG). The method of preparation used yielded polymersomes with an average diameter of 120 nm. Each polymersome was loaded with 58±8 SOD1 and 1270±200 CAT molecules (PS-PEG), or 60±10 SOD1 and 623±186 CAT molecules (PS-PIAT), respectively. This exceptionally high entrapment yield indicates at least a partial binding of the enzymes to the block-copolymers. Bottom: Experimental evidence for the functioning of the polymersome-confined SOD1/CAT systems – abbreviated as SOD,CAT-PS-PEG and SOD,CAT-PS-PIAT – as compared to the free enzymes (SOD,CAT) at the same overall enzyme concentrations. The formation of $O_2$ was measured during the first 400 s after chemical $O_2^{\bullet -}$ production in the bulk solution from PMS (phenazine methosulphate) and NADH (the reduced form of nicotinamide adenine dinucleotide). Although the free enzymes were more efficient, the experiments indicate that the polymersome-confined enzymatic cascade reactions also occurred. **b,** Protein capsule-confined enzymatic reaction, whereby the kinetic properties of the reaction are determined by the structure of the capsule shell[77]. Top: Schematic drawing on the preparation of the protein capsules. The capsule (diameter 27 nm) was assembled *in vitro* from 180 proteins in the presence of trimethylamine oxide (TMAO) and *E. coli* alkaline phosphatase, which carried a C-terminal sequence of 16 negatively charged amino acids (abbreviated as PhoA$^{WT}$–neg). This C-terminal sequence was used for the localization of the phosphatase inside the capsid on the basis of electrostatic interactions with positively charged residues on the capsid interior surface. The capsid shell contained pores with diameters of about 1.8 nm, allowing small molecules to migrate from the external bulk medium into the interior of the capsid, while folded proteins could not pass the pores. Bottom: The activity of the entrapped PhoA$^{WT}$–neg was measured for the wild type (WT) capsid as well as for different capsid mutants (KR, ED, E) pH = 8.0 with 4-methlyumelliferyl

phosphate (4-MUP). The products obtained were phosphate and 4-methylumbelliferone. The determined apparent Michaelis constant, $K_{M,app}$, and the catalytic constant, $k_{cat}$, varied with the electrostatic properties of the capsid shell. The WT capsid had a negative charge around the pore periphery but not inside the pore. Compared to the free enzyme, $k_{cat}$ of $PhoA^{WT}$–neg inside the WT capsid was lower, but the $K_{M,app}$ values were about the same. The mutants T71E (abbreviated as E) and T71E/V72D (abbreviated as ED) had significant negative charge throughout the pores; and mutant T71K/V72R (abbreviated as KR) had a positive charge in the pores. While the $k_{cat}$ values of the enzyme inside the mutant capsids with negatively charged pores (E and ED) were only slightly lower than $k_{cat}$ of the enzyme inside the WT capsid (comparison of v at high substrate concentrations), $K_{M,app}$ was significantly higher inside these capsid mutants, independent on the salt concentration. For the mutants with positively charged pores (KR), $k_{cat}$ of the entrapped enzyme was higher than for the enzyme inside the WT capsid; $K_{M,app}$ was about the same. **c,** Protein capsule-confined enzymatic reaction, whereby the three enzymes of a cascade reaction were encapsulated at a defined ratio[93]. Top: Schematic representation of the preparation of a bacteriophage P22 capsid (diameter 58 nm) containing the three enzymes CelB (red, a tetrameric galactosidase), GLUK (blue, a dimeric ADP-dependant β-glucokinase), GALK (green, a monomeric ATP-dependant galactokinase), and a scaffold protein domain (SP, purple). ① Genes were constructed for the expression of fusion proteins containing the three enzymes which were linked together through flexible spacer peptides. The coat protein (CP, grey) was expressed as well. ②Assembly of the three covalently linked enzymes to satisfy the properties of the native enzymes as tetramer (CelB) or dimer (GLUK). ③ The capsid formation is facilitated by the interaction of the SP domains and CP subunits, leading to the encapsulation of the multienzyme gene product. The capsid consisted of 420 CP monomers which assembled with the aid of about 300 SP monomers. The three enzymes catalyze a three-step cascade reaction (bottom): (1) hydrolysis of lactose to galactose and glucose (catalyzed by CelB); (2) phosphorylation of galactose in the presence of ATP by GALK to yield galactose-1-phosphate and ADP; (3) phsphorylation of glucose by GLUK with the formed ADP to yield glucose-6-phosphate and AMP. Left: Experimental evidence for the successful co-encapsulation of the three enzymes by analyzing the turnover of lactose to glucose-6-phosphate and galactose-1-phosphate upon addition of lactose and ATP. The turnover with all three enzymes was significantly higher than with CelB and GLUK only. Figures adapted

with minor modifications from: **a**, ref. 92, American Chemical Society; **b**, ref. 77, American Chemical Society; **c**, ref. 93, American Chemical Society.

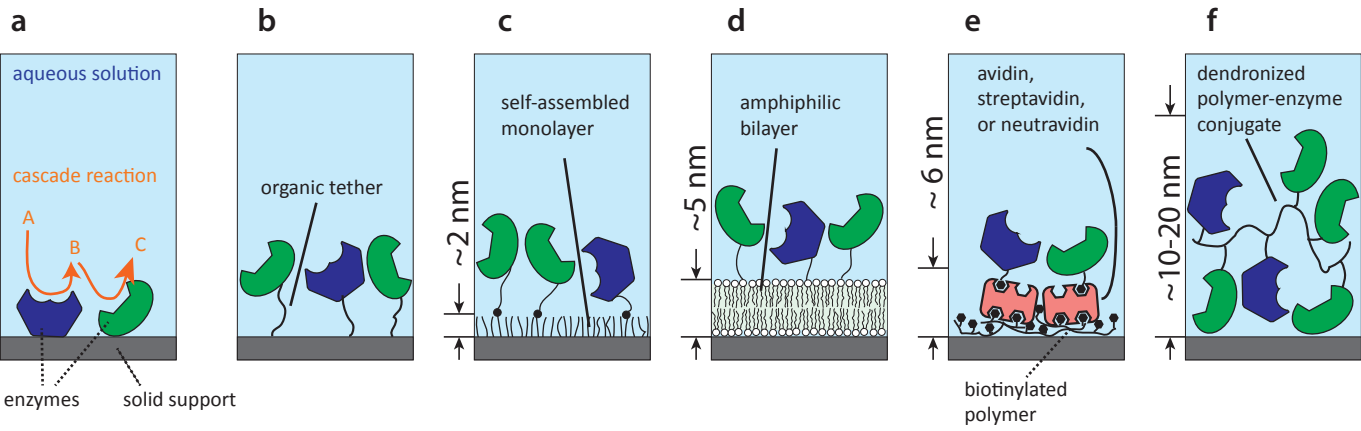
a
aqueous solution
cascade reaction
A
B
C
enzymes
solid support
b
organic tether
c
self-assembled
monolayer
~2 nm
d
amphiphilic
bilayer
~5 nm
e
avidin,
streptavidin,
or neutravidin
~ 6 nm
biotinylated
polymer
f
dendronized
polymer-enzyme
conjugate
~10-20 nm

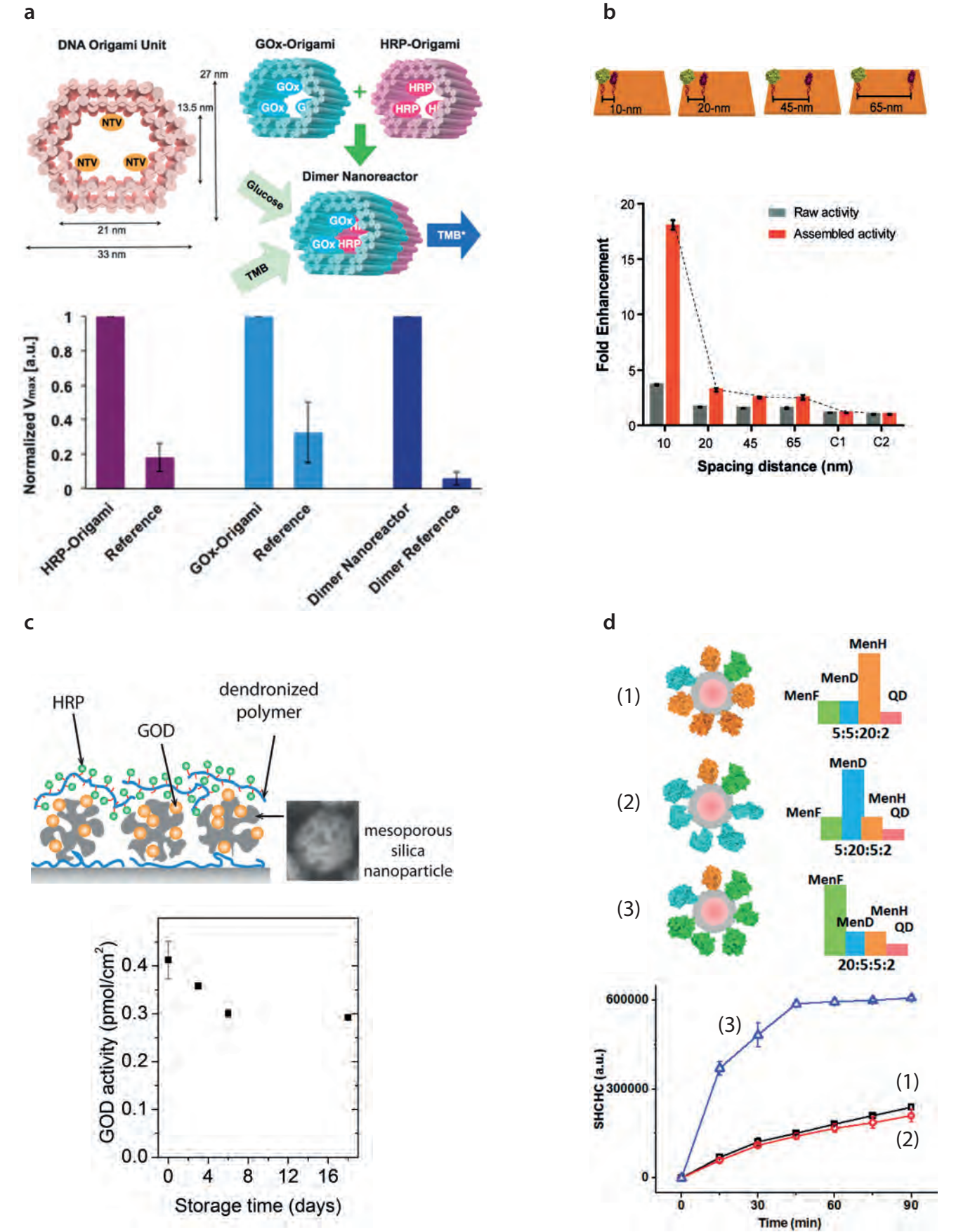
a
DNA Origami Unit
GOx-Origami
HRP-Origami
27 nm
13.5 nm
NTV
NTV
NTV
21 nm
33 nm
GOx
GOx
HRP
HRP
Dimer Nanoreactor
Glucose
TMB
TMB*
GOx
GOx
HRP
Normalized Vmax [a.u.]
1
0.8
0.6
0.4
0.2
0
HRP-Origami
Reference
GOx-Origami
Reference
Dimer Nanoreactor
Dimer Reference
b
10-nm
20-nm
45-nm
65-nm
Raw activity
Assembled activity
Fold Enhancement
20
15
10
5
0
10
20
45
65
C1
C2
Spacing distance (nm)
c
HRP
GOD
dendronized polymer
mesoporous silica nanoparticle
GOD activity (pmol/cm2)
0.4
0.3
0.2
0.1
0.0
0
4
8
12
16
Storage time (days)
d
(1)
MenH
MenD
MenF
QD
5:5:20:2
(2)
MenD
MenH
MenF
QD
5:20:5:2
(3)
MenF
MenH
MenD
QD
20:5:5:2
600000
300000
0
SHCHC (a.u.)
(3)
(1)
(2)
0
30
60
90
Time (min)

a

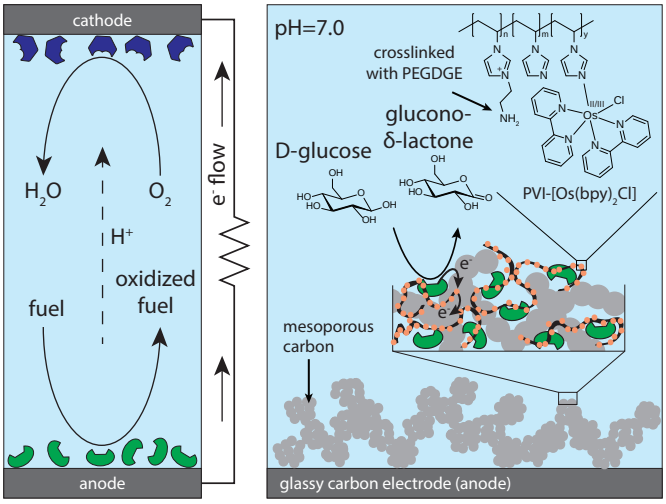
cathode
anode
$H_2O$
$O_2$
$H^+$
fuel
oxidized fuel
e⁻ flow
pH=7.0
crosslinked with PEGDGE
glucono-δ-lactone
D-glucose
PVI-[Os(bpy)2Cl]
mesoporous carbon
glassy carbon electrode (anode)

b

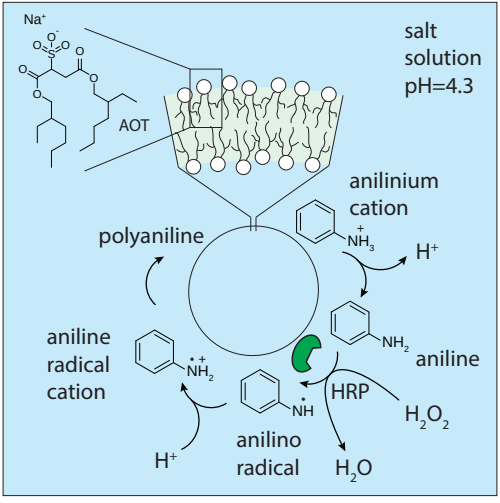
$Na^+$
AOT
salt solution pH=4.3
anilinium cation
polyaniline
$H^+$
aniline
HRP
$H_2O_2$
aniline radical cation
anilino radical
$H^+$
$H_2O$

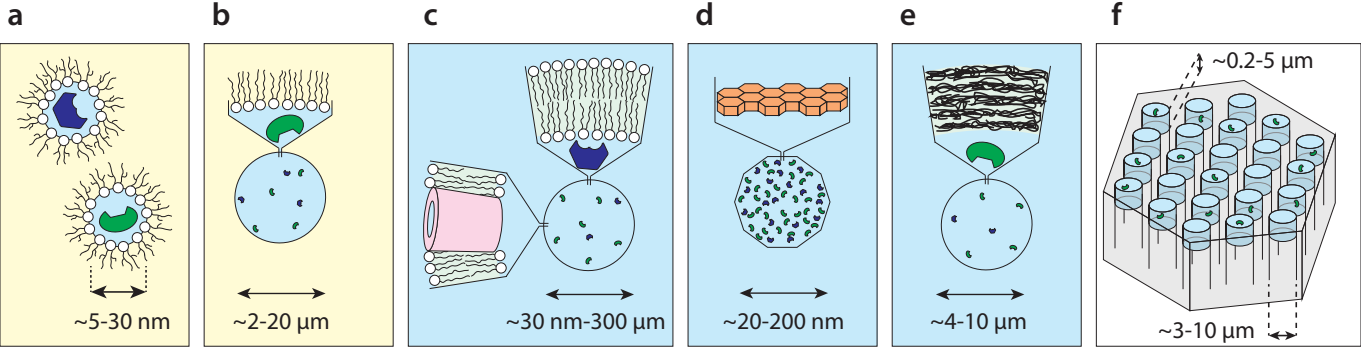
a
~5-30 nm
b
~2-20 µm
c
~30 nm-300 µm
d
~20-200 nm
e
~4-10 µm
f
~0.2-5 µm
~3-10 µm

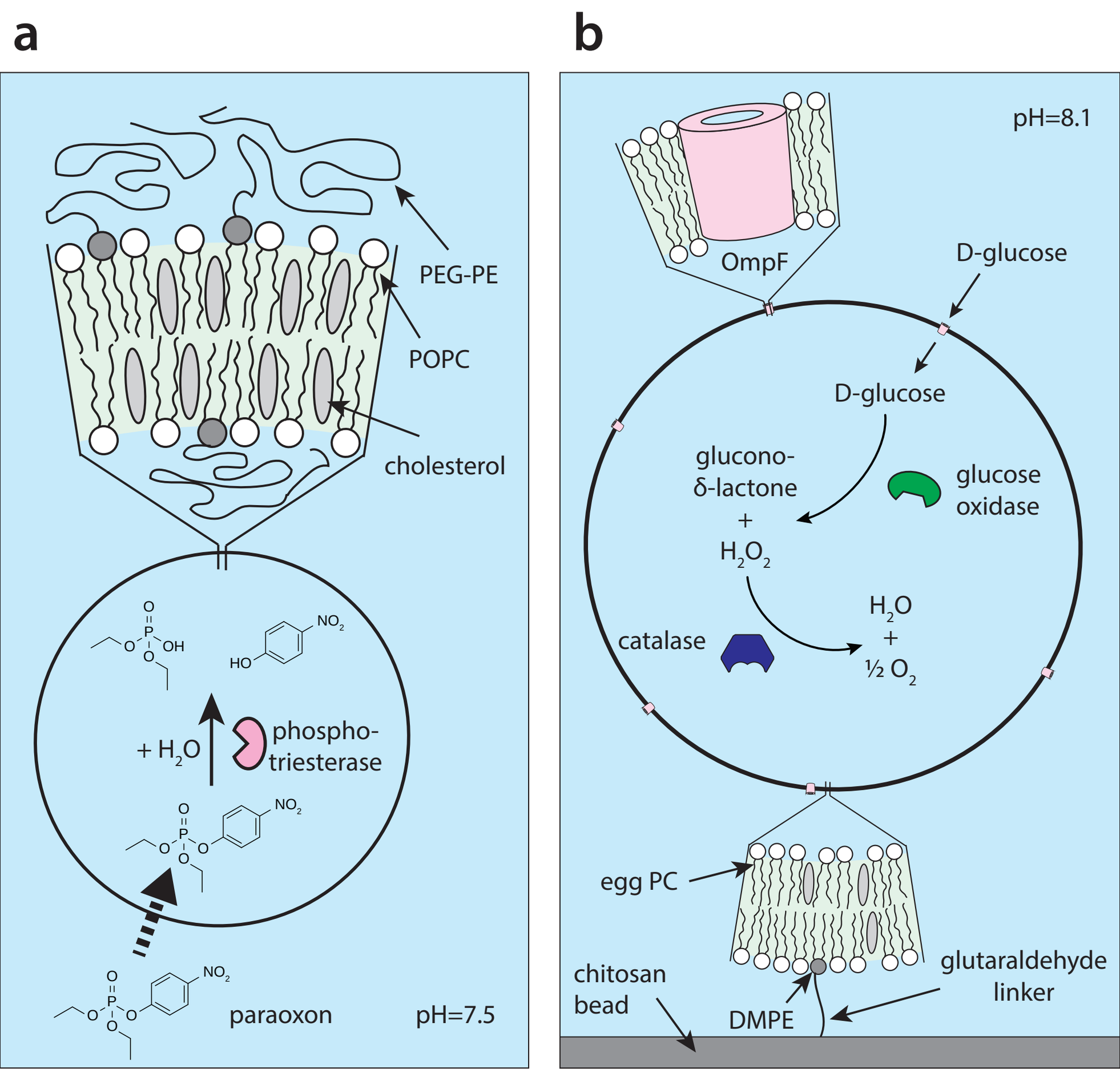
a
PEG-PE
POPC
cholesterol
+ H2O
phospho-
triesterase
paraoxon
pH=7.5
b
pH=8.1
OmpF
D-glucose
D-glucose
glucono-
δ-lactone
+
H2O2
glucose
oxidase
catalase
H2O
+
½ O2
egg PC
chitosan
bead
DMPE
glutaraldehyde
linker

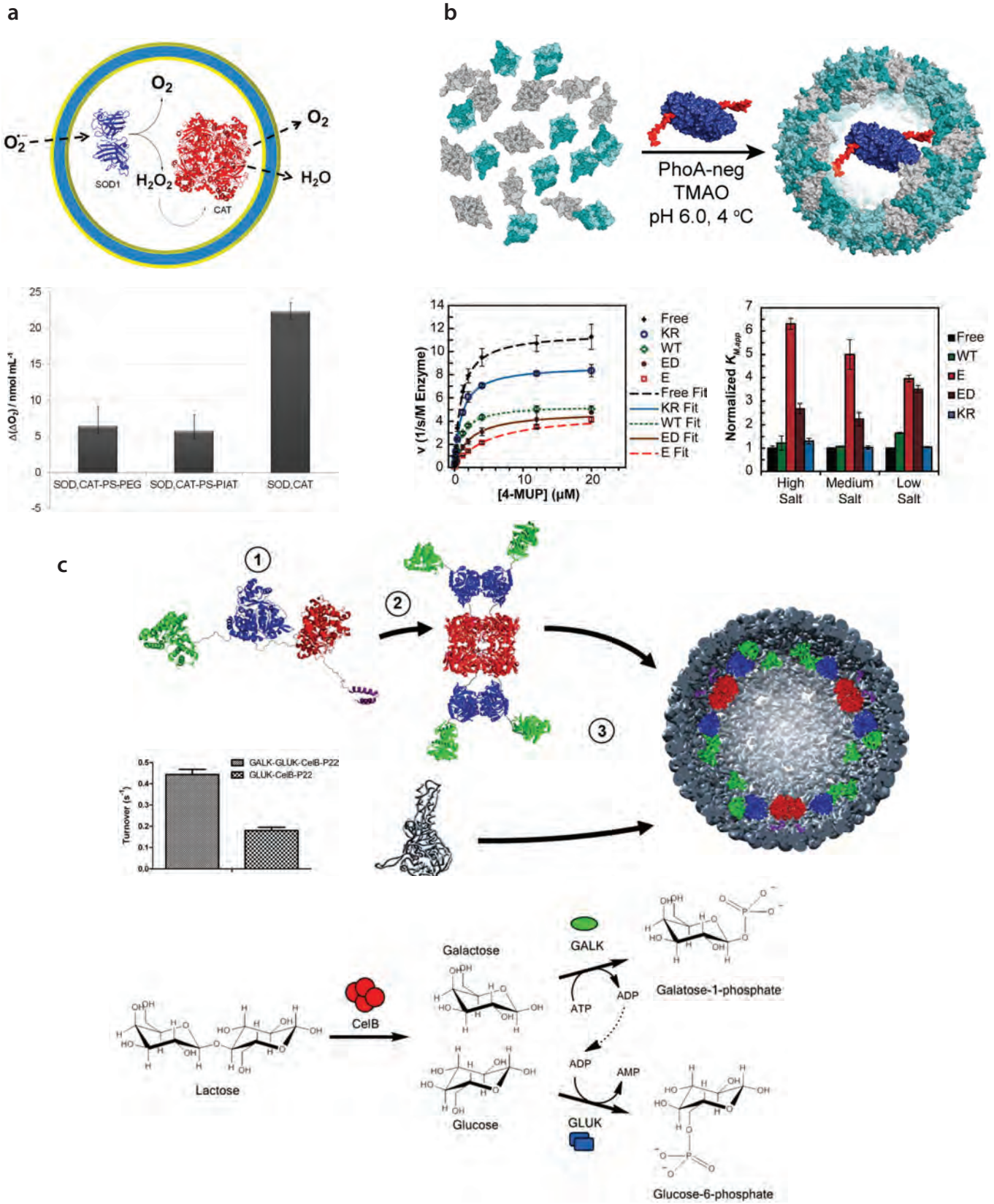
a
$O_2$
$O_2^{\cdot-}$
$O_2$
$H_2O_2$
$H_2O$
SOD1
CAT
b
PhoA-neg
TMAO
pH 6.0, 4 °C
Δ(ΔO2) / nmol mL-1
SOD,CAT-PS-PEG
SOD,CAT-PS-PIAT
SOD,CAT
v (1/s/M Enzyme)
[4-MUP] (μM)
Free
KR
WT
ED
E
Free Fit
KR Fit
WT Fit
ED Fit
E Fit
Normalized $K_{M,app}$
High Salt
Medium Salt
Low Salt
c
1
2
3
Turnover (s-1)
GALK-GLUK-CelB-P22
GLUK-CelB-P22
Lactose
CelB
Galactose
Glucose
GALK
ATP
ADP
Galatose-1-phosphate
ADP
AMP
GLUK
Glucose-6-phosphate